

Full Statistics of Regularized Local Energy Density in a Freely Expanding Kipnis-Marchioro-Presutti Gas

Eldad Bettelheim^{1,*} and Baruch Meerson^{1,†}

¹*Racah Institute of Physics, Hebrew University of Jerusalem, Jerusalem 91904, Israel*

We combine the Macroscopic Fluctuation Theory and the Inverse Scattering Method to determine the full long-time statistics of the energy density $u(x, t)$ averaged over a given spatial interval,

$$U = \frac{1}{2L} \int_{-L}^L dx u(x, t),$$

in a freely expanding Kipnis-Marchioro-Presutti (KMP) lattice gas on the line, following the release at $t = 0$ of a finite amount of energy at the origin. In particular, we show that, as time t goes to infinity at fixed L , the large deviation function of U approaches a universal form when expressed in terms of the energy content of the interval $|x| < L$ at time t . A key part of the solution is the determination of the most likely configuration of the energy density at time t , conditional on U .

I. INTRODUCTION AND MFT EQUATIONS

Stochastic lattice gases are simple, versatile and instructive models which capture universal aspects of large deviations of different fluctuating quantities (the density field, the integrated current, *etc.*) in macroscopic systems of interacting particles out of equilibrium [1–4]. The last two decades have witnessed a major progress in this area of nonequilibrium statistical mechanics. To a large extent, this progress has been made possible by the development of fluctuational hydrodynamics (FHD) [1] and macroscopic fluctuation theory (MFT) [5]. Stripped off irrelevant microscopic details, FHD and MFT are ideally suited for probing late-time asymptotic regimes which are usually the most interesting. This is especially true for non-stationary processes, where exact results for full statistics – by any method – are scarce [6–15].

Here we focus on the continuous-time Kipnis-Marchioro-Presutti (KMP) lattice gas model [16]. It involves immobile “agents” occupying a lattice and carrying continuous non-zero amounts of “energy”. At each random move a randomly chosen pair of nearest neighbors randomly redistributes their combined energy among them according to uniform distribution. The original motivation behind the KMP model was a rigorous proof of Fourier’s law of heat diffusion when starting from a microscopic model [16]. Since then the KMP model has been extensively studied in the context of nonequilibrium fluctuations of transport [7, 17–31].

In a parallel development, the last 15 years have witnessed significant interest and remarkable advancements [32–42] in the studies of the *one-point* statistics of the Kardar-Parisi-Zhang (KPZ) equation [43], a paradigmatic model of nonconservative nonequilibrium stochastic growth. An analogous one-point statistics in a stochastic lattice gas would be the statistics of the gas density (or temperature) at a specified point in space. It turns out, however, that in the continuum description of the conservative lattice gases, provided by the FHD, the one-point statistics is ill-defined, as the variance of the one-point fluctuations diverges at small scales. A similar ultraviolet catastrophe of the one-point fluctuations in nonequilibrium stochastic growth is well known to experts [44, 45]. It occurs in a broad family of continuous stochastic growth models when the dimension of space exceeds a model-dependent critical dimension [45]. Fortunately, for the KPZ equation the critical dimension is 2, which allows for unhindered studies of the one-point statistics in one dimension. For the lattice gases, however, the ultraviolet catastrophe occurs in all physical dimensions.

One remedy against the ultraviolet catastrophe is to introduce a small-scale cutoff: most naturally, the lattice constant. Such a regularization, however, would imply abandoning continuous theory with many of its benefits. An advantageous regularization alternative is to characterize local fluctuations by the probability distribution $\mathcal{P}(U, T)$ of the density or energy density averaged over a small but *macroscopic* spatial interval, $|x| < L$, at time $t = T$:

$$\frac{1}{2L} \int_{-L}^L dx u(x, t = T) = U. \quad (1)$$

* eldad.bettelheim@mail.huji.ac.il

† meerson@mail.huji.ac.il

This type of regularization was proposed in Ref. [45] for the stochastic surface growth. Here we apply it to a freely expanding KMP gas with a finite total energy W . Since we are interested in the long-time limit, $T \rightarrow \infty$, we may assume that the energy is initially released at a point, which we choose for simplicity to be $x = 0$:

$$u(x, t = 0) = W\delta(x). \quad (2)$$

The *expected* value of the locally averaged energy density U at the same point at time T ,

$$\bar{U} = \frac{\text{Werf}\left(\frac{L}{\sqrt{4T}}\right)}{2L}, \quad (3)$$

readily follows from the mean-field (that is, zero-noise) solution,

$$\bar{u}(x, t) = \frac{W}{\sqrt{4\pi t}} e^{-\frac{x^2}{4t}}, \quad (4)$$

of the diffusion equation $\partial_t \bar{u}(x, t) = \partial_x^2 \bar{u}(x, t)$ that governs the mean coarse-grained energy density of the KMP gas at long times [1, 3, 16]. Here we study fluctuations, including large deviations, of U around the expected value (3). In the long-time limit, $T \gg L^2$, the error function in Eq. (3) can be expanded at small argument, and we obtain

$$\bar{U} \simeq \frac{W}{\sqrt{4\pi T}}, \quad (5)$$

which is independent of the regularization length $2L$.

It is convenient to re-scale t , x and u by T , \sqrt{T} and W/\sqrt{T} , respectively. The initial condition (2) becomes

$$u(x, t = 0) = \delta(x), \quad (6)$$

while the condition (1) on the locally averaged density at $t = T$ can be written as

$$\int_{-\ell}^{\ell} dx u(x, t = 1) = \kappa \equiv 2\ell\nu, \quad (7)$$

where $\ell = L/\sqrt{T} \ll 1$. The quantity $\nu = U\sqrt{T}/W$ is the re-scaled regularized local energy density, while $\kappa = 2\ell\nu$ is the fraction of the total energy observed inside the interval $|x| < L$.

The (rescaled) optimal path of the process conditioned on U is described by the well-known MFT equations for the KMP model [5, 7]. They can be recast in the following symmetric form [10, 25]:

$$\partial_t u = \partial_x(\partial_x u + 2u^2 v), \quad (8)$$

$$\partial_t v = \partial_x(-\partial_x v + 2uv^2). \quad (9)$$

Equations (8) and (9) follow from a minimization of the action functional of a proper path integral, constrained by Eq. (7), with respect to variations of $u(x, t)$ [5, 7, 10, 25]. The minimization also yields, aside from Eqs. (8) and (9), a boundary condition at the (re-scaled) final time,

$$v(x, t = 1) = \lambda[\delta(x - \ell) - \delta(x + \ell)], \quad (10)$$

where λ is a Lagrange multiplier, to be ultimately expressed through ν and ℓ with the help of Eq. (7) [45]. Importantly, the MFT equations and boundary conditions for this problem obey the mirror symmetry and antisymmetry relations

$$u(-x, t) = u(x, t) \quad \text{and} \quad v(-x, t) = -v(x, t). \quad (11)$$

Once $u(x, t)$ and $v(x, t)$ have been found, one can calculate the rescaled action s [7, 25]

$$s = \int_0^1 dt \int_{-\infty}^{\infty} dx u^2(x, t) v^2(x, t) = 2 \int_0^1 dt \int_0^{\infty} dx u^2(x, t) v^2(x, t). \quad (12)$$

It is often simpler, however, to determine the action by using the ‘‘shortcut relation’’

$$\frac{ds}{d\kappa} = \lambda(\kappa), \quad (13)$$

which follows from κ and λ being conjugate variables, see *e.g.* Ref. [46]. The action gives the desired probability distribution \mathcal{P} up to a sub-leading, pre-exponential factor that we do not attempt to evaluate:

$$\ln \mathcal{P}(U, T, \ell) \simeq -\sqrt{T} s(\nu, \ell). \quad (14)$$

Since $\sqrt{T} \gg 1$, Eq. (14) clearly has a large-deviation structure, with the re-scaled action $s(\nu, \ell)$ playing the role of a rate function.

The main objective of this work is to determine the large-deviation function $s(\nu, \ell)$ in the leading order in the small regularization parameter ℓ but for arbitrary ν . In Sec. II we describe typical, small fluctuations of ν around its expected value $\bar{\nu} = \bar{U}\sqrt{T}/W$. Here one can use the Lagrange multiplier λ as a small expansion parameter [22]. We also present in Sec. II a free-energy argument that, as we argue, applies in a broad range of the densities ν . In Sec. III we apply the Inverse Scattering Method to obtain important relations which enable us to determine the complete rate function $s(\nu, \ell)$, to justify the free-energy argument and establish its applicability limits, and to find additional asymptotics of the rate function. In particular, we show that, in the limit of $\ell \rightarrow 0$, the rate function expressed in terms of $\kappa = 2\ell\nu$ acquires a universal (ℓ -independent) form. We also present two instructive examples of the optimal configurations $u(x, 1)$ at different λ (or ν). Section IV briefly summarizes and discusses our results.

II. LINEAR THEORY AND FREE-ENERGY ARGUMENT

Typical fluctuations of ν around its expected value $\bar{\nu} = \bar{U}\sqrt{T}/W$ are Gaussian. Here one can linearize Eqs. (8) and (9) with respect to $|\lambda| \ll 1$ [22]. Then Eq. (9) becomes simply $\partial_t v = -\partial_x^2 v$. This anti-diffusion equation can be solved backward in time with the “initial” condition (10). The solution, for arbitrary ℓ , is

$$v(x, t) = \frac{\lambda}{\sqrt{4\pi(1-t)}} \left[e^{-\frac{(x-\ell)^2}{4(1-t)}} - e^{-\frac{(x+\ell)^2}{4(1-t)}} \right]. \quad (15)$$

The action s in the leading (second) order in λ can be obtained from Eq. (12) by using the solution (15) for $v(x, t)$ and setting $u(x, t) = \bar{u}(x, t)$ from (a re-scaled) Eq. (4). Evaluating the double integral, we arrive at the following expression:

$$s(\lambda, \ell) = \frac{\lambda^2}{4\sqrt{2\pi}} \left[e^{-\frac{\ell^2}{2}} - \operatorname{erfc} \left(\frac{\ell}{\sqrt{2}} \right) \right]. \quad (16)$$

Then, using the shortcut relation (13), we can express the re-scaled action in terms of ν :

$$s(\nu, \ell) = \frac{4\sqrt{2\pi}\ell^2 e^{\frac{\ell^2}{2}}}{1 - e^{\frac{\ell^2}{2}} \operatorname{erfc} \left(\frac{\ell}{\sqrt{2}} \right)} (\nu - \bar{\nu})^2, \quad (17)$$

where

$$\bar{\nu} \equiv \frac{\bar{U}\sqrt{T}}{W} = \frac{1}{2\ell} \operatorname{erf} \left(\frac{\ell}{2} \right), \quad (18)$$

and the validity of the linear theory requires that $|\nu - \bar{\nu}| \ll \bar{\nu}$.

For $\ell \ll 1$, that is at sufficiently long time at fixed L , Eqs. (17) and (18) simplify to

$$s(\nu, \ell) \simeq 4\pi\ell (\nu - \bar{\nu})^2 \quad (19)$$

and

$$\bar{\nu} \simeq \frac{1}{\sqrt{4\pi}}, \quad (20)$$

respectively. The variance of fluctuations of ν is equal to $1/(8\pi\ell)$. It diverges in the limit of $\ell \rightarrow 0$, exhibiting the ultraviolet catastrophe [45]. The $1/\ell$ scaling of the variance is to be expected. Indeed, the final re-scaled energy density inside the small interval $|x| < \ell$ is already almost constant and equal to $1/(8\pi\ell)$. In its turn, the variance of ν scales as one over the energy content of this interval.

For future reference, the small- ℓ asymptotic of the action (16) in terms of λ is

$$s(\lambda, \ell \ll 1) = \frac{\ell \lambda^2}{4\pi}. \quad (21)$$

Alongside with the shortcut relation (13), this again leads to the small- ℓ asymptotic (19).

When ℓ is small, the linear theory predicts a flat optimal density profile at the observation time in the ‘‘interior region’’ $|x| \ll \ell$:

$$u(|x| < \ell, t = 1) = \frac{1}{\sqrt{4\pi}} + \frac{\lambda}{4\pi} + \dots, \quad (22)$$

where the ellipsis denotes sub-leading corrections in $\ell \ll 1$. By assuming a flat density profile $u(|x| < \ell, 1) = \nu$ from the start, one can obtain Eq. (22) from Eqs. (13), (19) and (20).

Importantly, at $\ell \ll 1$, the gas in the small interior region $|x| < \ell$ has a sufficient time to reach thermal equilibrium [45]. It is not surprising, therefore, that the Gaussian asymptotic (21), and hence (19), for the action also follows from the Boltzmann-Gibbs free energy difference [7, 22]

$$s \simeq \int_{-\ell}^{\ell} dx [F(u(x, 1)) - F(\bar{u}) - F'(\bar{u})(u(x, 1) - \bar{u})], \quad (23)$$

where $F(u) = -\ln u$ is the equilibrium free energy density of the KMP gas, see e.g. Refs. [7, 22]. To see it, one should set in Eq. (23) $\bar{u} = \bar{\nu} = 1/\sqrt{4\pi}$, use Eq. (22) for $u(|x| < \ell, 1)$ and expand the integrand in powers of λ up to, and including, a quadratic term.

As we will show in Sec. III A, at $\ell \ll 1$ Eq. (23) actually holds well beyond the linear theory, once the density at the final time $t = 1$ is approximately uniform in the interior region: $u(|x| < \ell, 1) = \text{const} = \nu$. In this case Eq. (23) predicts

$$s_{\text{equil}}(\nu, \ell) \simeq 2\ell \left(\frac{\nu}{\bar{\nu}} - \ln \frac{\nu}{\bar{\nu}} - 1 \right). \quad (24)$$

Notice that the rate function (24) diverges logarithmically at $\nu \rightarrow 0$. This important property is characteristic of the KMP gas, and it can be traced down to the nature of its microscopic model, which deals with a continuous energy variable rather than discrete particles.

III. SOLUTION BY THE INVERSE SCATTERING METHOD

As was noticed in Ref. [10], the MFT equations (8) and (9) formally coincide with the derivative nonlinear Schrödinger equation (DNLS) in imaginary space and time. Application of the Inverse Scattering Method (ISM) to the DNLS was pioneered by Kaup and Newell [47] for initial-value problems. Adaptation of the method to boundary-value problems in time has been described in detail in several papers [10, 13–15]. Nevertheless, we outline here the main steps of the method, as it applies to the current problem, forgoing a derivation of Eq. (28) below, and skipping some of the actual calculations, as they can be easily recovered. Following Kaup and Newell [47], one starts with the auxiliary scattering problem for the field $\psi(x, t; k)$,

$$\partial_x \psi(x, t; k) = V(x, t; k) \psi(x, t; k), \quad (25)$$

where

$$V(x, t; k) = \begin{pmatrix} -\frac{\zeta^2}{2} & -iv(x, t)\zeta \\ -iu(x, t)\zeta & \frac{\zeta^2}{2} \end{pmatrix} \quad (26)$$

and $\zeta = \sqrt{ik}$. The variable k is a wave number describing the plane-wave boundary conditions at $x \rightarrow \infty$ for $\psi(x, t; k)$, while the t -dependence comes into play in the form of dependence of V on t through u and v . Namely, one assumes $\psi(x, t; k) = \begin{pmatrix} \alpha e^{-ikx} \\ \beta e^{ikx} \end{pmatrix}$ at $x \rightarrow -\infty$. Then, using the linearity of the problem and the form of the solution at infinity, where u and v vanish, one obtains the following asymptotic behavior at $x \rightarrow +\infty$:

$$\psi(x, t; k) = \begin{pmatrix} \alpha a(k; t) e^{-ikx} + \beta \tilde{b}(k; t) e^{-ikx} \\ \alpha b(k; t) e^{ikx} + \beta \tilde{a}(k; t) e^{ikx} \end{pmatrix}. \quad (27)$$

The integrability of the problem manifests itself in the fact that the time evolution of the parameters a , \tilde{a} , b and \tilde{b} is very simple:

$$a(k; t) = a(k; 0), \quad \tilde{a}(k; t) = \tilde{a}(k, 0), \quad e^{k^2 t} b(k, t) = b(k, 0), \quad \text{and} \quad \tilde{b}(k, t) = \tilde{b}(k, 0) e^{k^2 t}. \quad (28)$$

These relations, alongside with the fact that $a(k; t)$ is analytic in the upper half k -plane, while $\tilde{a}(k; t)$ is analytic in the lower half plane [47], allows one to find explicit expressions for $v(x, 0)$ and $u(x, 1)$, as we shall see below.

Now we proceed to calculating $\tilde{b}(k; 0)$ and $\tilde{a}(k; 0)$ by solving the scattering problem, Eq. (25), at time $t = 0$ setting $\alpha = 0$ and $\beta = 1$. The solution of the scattering problem is greatly aided by the fact that $u(x, 0) = \delta(x)$, see Eq. (10). We obtain

$$\tilde{b}(k; 0) = -i\zeta [Q(k) - ikQ_+(k)Q_-(k)] \quad \text{and} \quad \tilde{a}(k; 0) = 1 - ikQ_-(k), \quad (29)$$

where

$$Q_+(k) = \int_0^\infty e^{\zeta^2 x'} v(x') dx', \quad Q_-(k) = \int_{-\infty}^0 e^{\zeta^2 x'} v(x') dx' \quad \text{and} \quad Q(k) = Q_+(k) + Q_-(k). \quad (30)$$

A similar exercise can be performed at $t = 1$, this time making use of the simple form of $v(x, 1)$ given by Eq. (10) to solve the scattering problem, Eq. (25). However, in order to carry out this calculation, one must first make some assumptions about the behavior, in the limit of $\ell \rightarrow 0$ that we are interested in, of $u(x, 1)$ in the two natural regions that space is divided into due to the form of $v(x, 1)$, namely the interior region $|x| < \ell$ and the exterior region $|x| > \ell$. We make the following assumption, to be validated a posteriori. We assume that, as $\ell \rightarrow 0$, the quantity $u(x, 1)\ell$ in the interior region $|x| < \ell$ converges to a certain finite x -independent value $u_0\ell$. (We will ultimately identify the quantity u_0 with ν). Because of the shocks of $u(x, 1)$ at $|x| = \ell$, the value of u_0 is different from the limiting value of $u(x, 1)$ as $x \rightarrow \pm(\ell + 0^+)$. We denote the latter by u_\pm . Let us also denote by v_\pm the limiting values of $v(x, 0)$ as $x \rightarrow 0^\pm$. We show in the following, the quantities v_\pm actually vanish, but we do not assume it a priori. We summarize these definitions here:

$$u_0 = \ell^{-1} \lim_{\ell \rightarrow 0} \ell u(x, 1) \text{ for } |x| < \ell, \quad u_\pm = u[x \pm (\ell + 0^\pm), 1], \quad v_\pm = v(x \pm 0^\pm, 0). \quad (31)$$

We also remind the reader that $u(x, 1)$ is mirror symmetric with respect to x , while $v(x, 0)$ is antisymmetric, see Eq. (11).

Performing the scattering transform at $t = 1$ and using the small parameter $\ell \ll 1$, we arrive at the following relations:

$$\tilde{b}(k; 1) = 2\lambda(\lambda u_0 + 1)\zeta \sin(k\ell) \simeq -2i\lambda\ell\zeta^3(\lambda u_0 + 1), \quad (32)$$

$$\tilde{a}(k; 1) = 1 - 2\lambda\ell ik u_0 - 2\lambda\ell k^2(1 + \lambda u_0) \int_\ell^\infty e^{-ikx} u(x, 1) dx. \quad (33)$$

Now, using Eq. (28) to compare of $\tilde{a}(k; t)$ at $t = 0$ and $t = 1$, we obtain

$$2\lambda\ell u_0 - 2\lambda\ell ik(1 + \lambda u_0) \int_\ell^\infty e^{-ikx} u(x, 1) dx = - \int_{-\infty}^0 e^{ikx} v(x, 0) dx. \quad (34)$$

Setting $k = 0$, we obtain

$$u_0 = -\frac{1}{2\lambda\ell} \int_{-\infty}^0 v(x, 0) dx \equiv \frac{1}{2\lambda\ell} \int_0^\infty v(x, 0) dx. \quad (35)$$

Sending k to ∞ , we observe that the dominant contribution to the integral over x on the l.h.s. comes from a narrow region of width $O(1/k)$ near $x = \ell$. In this narrow region one can replace $u(x, 1)$ by u_0 . The integral over x on the r.h.s. vanishes in the leading order as $k \rightarrow \infty$, and we obtain

$$u_0 = u_+(1 + \lambda u_0). \quad (36)$$

Now we rewrite $-ike^{-ikx}$ on the l.h.s of Eq. (34) as $\partial_x e^{-ikx}$, perform integration by parts, and send ℓ to 0 in the leading order in small ℓ . Then we use Eq. (36), observe a cancellation of two terms and perform inverse Fourier transform of the both sides of the equation. We obtain the following relation between $u(x, 1)$ and $v(x, 0)$:

$$v(x, 0) = -2\lambda\ell(1 + \lambda u_0)\partial_x u(x, 1), \quad (37)$$

In a similar way, by comparing \tilde{b} at $t = 0$ and $t = 1$, one obtains the relation

$$-i\zeta(Q - ikQ_+Q_-) = -i\zeta^3 2\lambda\ell(1 + \lambda u_0), \quad (38)$$

which can be recast in the following form:

$$(1 - ikQ_+)(1 - ikQ_-) = 1 + 2\lambda\ell(1 + \lambda u_0)k^2 e^{-k^2}. \quad (39)$$

Noticing that the quantities $1 - ikcQ_{\pm}$ are analytic in the upper and lower half k -planes respectively, we recognize this equation as the decomposition of the function on the right hand side into a product of functions analytic in the upper and lower half planes, respectively. It is then natural to take the logarithm of this equation. This is facilitated by the following definition of M_{\pm} :

$$1 - ikQ_{\pm}(k) = (1 \pm v_{\pm})e^{M_{\pm}}, \quad (40)$$

where one recognizes in M_{\pm} the logarithm of $1 - ikQ_{\pm}$, respectively, but up to a constant, which is given by $(1 + v_{\pm})$, where v_{\pm} are defined in Eq. (31). These factors allow one to define M_{\pm} as functions which go to 0 as $k \rightarrow \infty$. Then, taking this limit on both sides of Eq. (40), one can see that on the left hand side one obtains $1 \pm v_{\pm}$ as a consequence of the definition of $Q_{\pm}(k)$, Eq. (30). The right hand side is then decorated by the factors $1 \pm v_{\pm}$ in order to match this asymptotic.

The decomposition of the logarithm of the right hand side of Eq. (39) into M_{\pm} , which in turn is the logarithm (up to a constant) of $1 - ikQ_{\pm}$, is performed in the usual way to give the following result:

$$M_{\pm} = \pm \int_{-\infty}^{\infty} \frac{\ln\left(1 + 2\lambda\ell(1 + \lambda u_0)k^2 e^{-k'^2}\right) dk'}{k - k' \mp i0^+} \frac{dk'}{2\pi i} \quad (41)$$

which yields an expression for Q_{\pm} :

$$ikQ_{\pm}(k) = 1 - (1 \pm v_{\pm}) \exp \left[\pm \int_{-\infty}^{\infty} \frac{\ln\left(1 + 2\lambda\ell(1 - \lambda u_0)k^2 e^{-k'^2}\right) dk'}{k' - k \mp i0^+} \frac{dk'}{2\pi i} \right]. \quad (42)$$

Since Q_{\pm} is the Fourier transform of $\theta(\pm x)v(x, 0)$, respectively, this equation alongside with Eq. (37) gives $v(x, 0)$ and $u(x, 1)$, provided that v_{\pm} and u_0 are found.

The quantities v_{\pm} can be found from a demand that $Q_{\pm}(k)$ be regular at the origin. This is equivalent to a demand that $u(x, 1)$ tend to zero at infinity, which in our problem is satisfied automatically. Setting $k = 0$ in Eq. (42), one can see that the quantities v_{\pm} , defined in Eq. (31), vanish, and the factors $1 + v_{\pm}$ in Eq. (42) are both equal to 1. Combining Eqs. (30), (42) and (35), we arrive at a transcendental equation for $u_0 = \nu$:

$$4\pi\lambda\ell\nu = \int_{-\infty}^{\infty} \frac{\ln\left[1 + 2\lambda\ell(1 + \lambda\nu)k^2 e^{-k^2}\right]}{k^2} dk. \quad (43)$$

Equations (42) (with $v_{\pm} = 0$) and (43) yield $v(x, 0)$, while the relationship (37) between $v(x, 0)$ and $\partial_x u(x, 1)$, allows one to find $u(x, 1)$ as well. In fact, Eq. (43), combined with the ‘‘shortcut relation’’ (13), suffice for the purpose of calculating the action $s(\nu, \ell)$ which serves as the rate function of the probability density $\mathcal{P}(U, T, \ell)$, see Eq. (14).

A. Rate function and its asymptotics

For general λ , Eq. (43) for ν can only be solved numerically. As an example, the left panel of Fig. 1 shows a fragment of the resulting dependence of ν upon λ for $\ell = 0.01$. The point $\lambda = 0$ corresponds to $\nu = \bar{\nu} = 1/\sqrt{4\pi}$, as to be expected. The right panel of Fig. 1 shows the rate function $s(\nu)$ obtained from Eq. (13) by integrating numerically the inverse function $\lambda(\nu)$. The inset compares this $s(\nu)$ with predictions from the linear theory, Eq. (19), and from the free-energy difference, Eq. (24). As one can see, the Gaussian asymptotic, predicted by the linear theory, applies only in a narrow region of ν around $\bar{\nu}$, whereas the free-energy difference captures $s(\nu)$ in a much broader range of ν .

To understand the formal reason behind the latter finding, we notice that, because of the factor e^{-k^2} of the integrand in Eq. (43), the characteristic width of the integration region in k is $O(1)$. Let us assume (and check a posteriori) that

$$2|\lambda\ell(1 + \lambda\nu)| \ll 1, \quad (44)$$

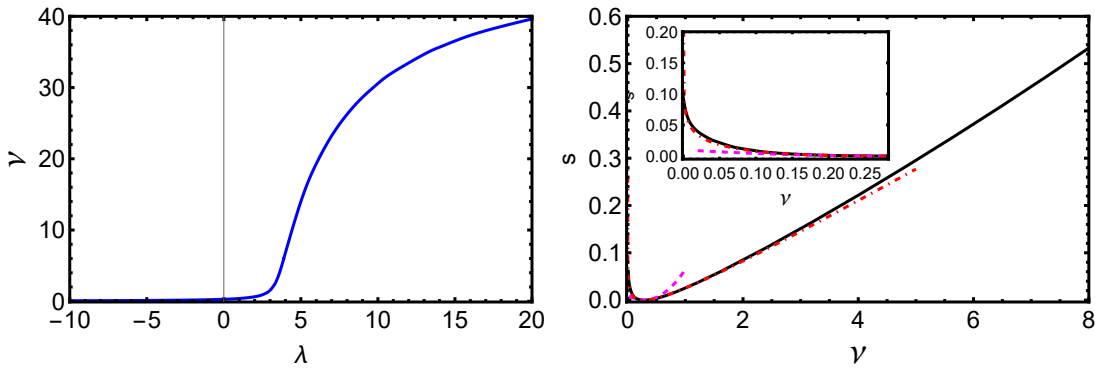


FIG. 1. Left panel: $\nu = \nu(\lambda)$, found by numerically solving Eq. (43) for $\ell = 0.01$ and different λ . Right panel: the rate function s vs. ν for this ℓ (the solid line), the linear theory prediction (19) (the dashed line) and the prediction from the free-energy difference (24) (the dot-dashed line). The inset shows a blowup of the interval $0 < \nu < \bar{\nu}$.

and expand the logarithm keeping only the linear term: $\ln \left[1 + 2\lambda\ell(1 + \lambda\nu)k^2e^{-k^2} \right] \simeq 2\lambda\ell(1 + \lambda\nu)k^2e^{-k^2}$. Evaluating the elementary integral and solving the resulting simple algebraic equation for ν , we obtain

$$\nu = \frac{1}{\lambda_c - \lambda}, \quad \text{where} \quad \lambda_c = \sqrt{4\pi} \equiv 1/\bar{\nu}. \quad (45)$$

Integrating Eq. (13) with $\kappa = 2\ell\nu = 2\ell/(\lambda_c - \lambda)$, we reproduce the free-energy prediction (24). As we already discussed, the Gaussian asymptotic (19), predicted by linear theory, is a particular limit of Eq. (24), only valid in the vicinity of $\nu = \bar{\nu}$. To obtain this asymptotic directly from Eq. (43), one should expand the integrand in the powers of λ up to and including the second order, and keep only the leading (first-order) term in $\ell \ll 1$.

Importantly, for Eq. (45) to make sense, λ must obey the condition

$$-\infty < \lambda < \lambda_c. \quad (46)$$

In addition, the assumed strong inequality (44) can be justified only if λ is not too close to λ_c : $\lambda_c - \lambda \gg \ell$. As a result, the free-energy prediction (24) for the rate function applies for all ν much smaller than $O(1/\ell) \gg 1$.

What happens at $\nu \gtrsim O(1/\ell)$? Here the rate function can be determined numerically, as shown in Fig. 1. However, an important simplification occurs as $\ell \rightarrow 0$. As can be checked a posteriori, here the term $\lambda\nu$ inside the parentheses in Eq. (43), is much larger than 1. Neglecting this 1 in the zeroth order in ℓ at fixed $\kappa = 2\ell\nu$, one arrives at a universal equation for $\kappa = 2\ell\nu$ versus λ :

$$2\pi\lambda\kappa = \int_{-\infty}^{\infty} \frac{\ln \left(1 + \lambda^2\kappa k^2 e^{-k^2} \right)}{k^2} dk. \quad (47)$$

The resulting function $\kappa(\lambda)$, obtained numerically, is shown on the left panel of Fig. 2. In this limit $\kappa(\lambda)$ vanishes at $\lambda < \lambda_c$, and it undergoes a tangent bifurcation at $\lambda = \lambda_c$. The right panel shows the resulting universal rate function $s_{>}(\kappa)$ alongside with its two asymptotics: $s_{>}(\kappa \rightarrow 0) \simeq \sqrt{4\pi}\kappa$, and the asymptotic at $\kappa \rightarrow 1$. Importantly, the $\kappa \rightarrow 0$ asymptotic matches the $\nu \gg \bar{\nu}$ asymptotic of the equilibrium rate function, which is described by the first term in the r.h.s. of Eq. (24).

The asymptotic at $\kappa \rightarrow 1$ can be expressed in terms of product log (Lambert W) function, very similarly to how it has been done in Ref. [10]. Alternatively, it can be presented in a parametric form as follows:

$$\kappa(\lambda \rightarrow \infty) \simeq 1 - \frac{6\sqrt{\ln \lambda}}{\pi\lambda}, \quad s_{>}(\lambda \rightarrow \infty) \simeq \frac{4(\ln \lambda)^{3/2}}{\pi}. \quad (48)$$

When ℓ is small but finite, the tangent bifurcation at $\lambda = \lambda_c$ is smoothed out, and κ is non-zero even for $\lambda < \lambda_c$. However, as ℓ is reduced, the functions $\kappa(\lambda, \ell)$, calculated from Eq. (43) for different ℓ , converge to the universal curve $\kappa(\lambda)$. This convergence is evident in Fig. 3: at $\ell = 10^{-4}$ the function $\kappa(\lambda, \ell)$ is already almost indistinguishable from the universal curve shown in the inset of the left panel of Fig. 2.

Now we are in a position to examine the validity of our analytical results. The main assumption we made in order to arrive at Eqs. (32) and (33) is that, to a leading order in ℓ , the integral $\int_{-\ell}^{\ell} e^{-ikx}u(x, 1)$ is independent of k in the

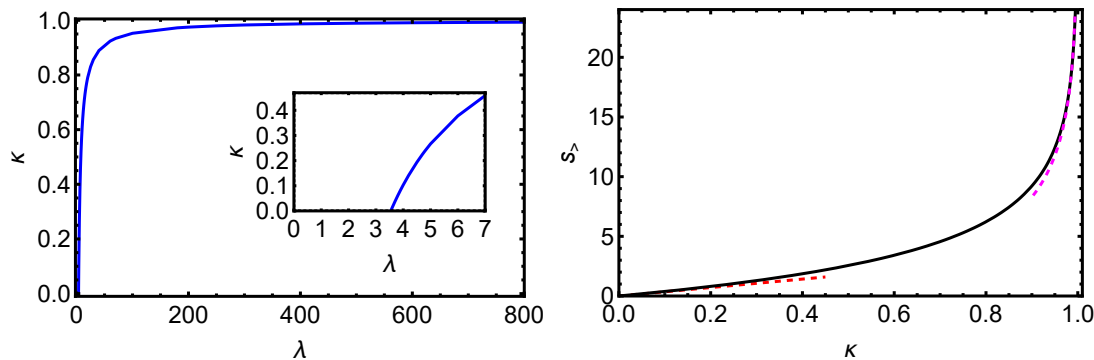


FIG. 2. Left panel: $\kappa = 2\ell\nu$ versus λ , found by numerically solving the universal equation (45). The inset focuses on the region close to the tangent bifurcation point $\lambda = \lambda_c = \sqrt{4\pi}$. Right panel: the rate function $s_{>}(\kappa)$ in terms of the energy fraction κ alongside with its small- κ asymptotic $s_{>}(\kappa \rightarrow 0) \simeq \sqrt{4\pi}\kappa$, and the large- κ asymptotic (48).

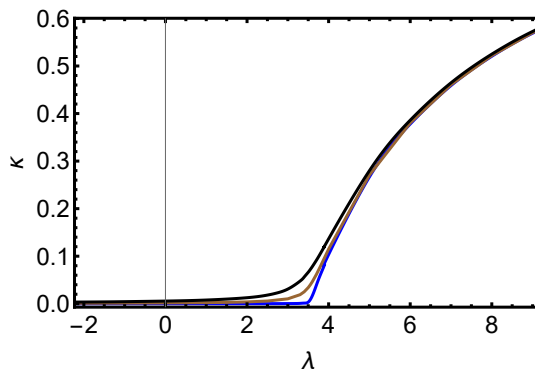


FIG. 3. Convergence of $\kappa(\lambda, \ell)$ to the universal function $\kappa(\lambda)$ for $\ell = 10^{-2}$, $3 \cdot 10^{-3}$ and 10^{-4} (from top to bottom).

relevant range of k in the problem, and therefore it can be approximated by $2\nu\ell$. This requires that the characteristic length scale of $u(x, 1)$, which is $O(\ell)$, be much smaller than the relevant $1/k$. The latter is determined by the effective width of the integration region in Eq. (43). For $-\infty < \lambda < \lambda_c$, ν is given by Eq. (45). As one can check, in this case the relevant range of k is $O(1)$, and the strong inequality $\ell \ll 1$ suffices.

For $\lambda \gtrsim \lambda_c$ an additional condition appears. This is because in this case we obtain $\nu\ell \simeq 1$. As a result, the effective width of the integration region over k in Eq. (43) is $O(\sqrt{\ln \lambda^2})$. This quantity should be much smaller than $1/\ell$:

$$\ell\sqrt{\ln \lambda^2} \ll 1. \quad (49)$$

This condition invalidates the rate function, that we found here, when κ becomes too close to its (unreachable) maximum possible value 1.

B. Optimal density configurations at $t = 1$

As we have seen, the ISM also predicts the optimal density profile $u(x, 1)$ and the optimal profile of the conjugate field $v(x, 0)$, see Eqs. (37), (42) and (43). Two examples of the optimal density profiles at $t = 1$ for $\lambda = 10$ and $\lambda = -30$ are shown in Fig. 4. For comparison, also shown is the expected, that is mean-field, density profile $e^{-x^2/4}/\sqrt{4\pi}$.

IV. SUMMARY AND DISCUSSION

By combining the MFT and the ISM, we calculated the long-time large-deviation statistics of the locally-averaged energy density in a freely expanding Kipnis-Marchioro-Presutti lattice gas. We showed that the corresponding rate function exhibits two distinct regions. One region corresponds to relatively small local densities and is described

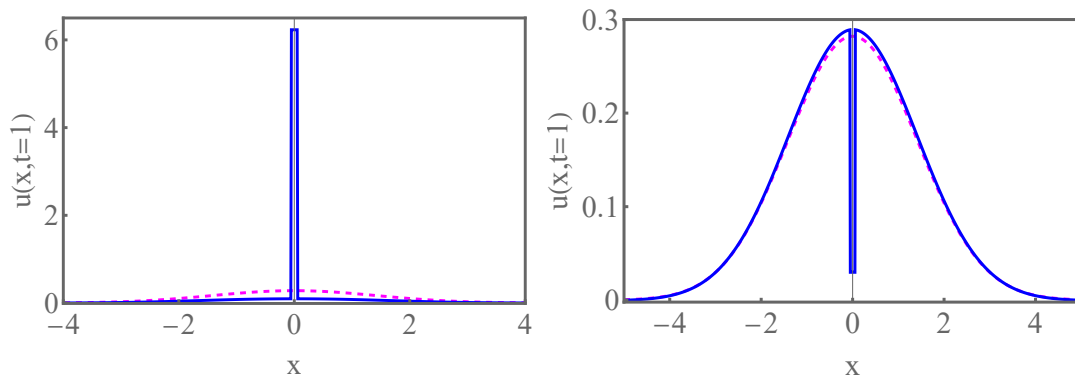


FIG. 4. Solid lines: $u(x, 1)$ for $\lambda = 10$ (left panel) and -30 (right panel) as described by the ISM for $\ell = 0.05$. Dashed lines: the expected density profile $(4\pi)^{-1/2}e^{-x^2/4}$. Note the different vertical scales.

by the equilibrium free-energy argument. The other region, associated with large densities, is fundamentally non-equilibrium. As time increases at a fixed L , the rate function converges to a universal form when expressed in terms of the energy content of the interval $|x| < \ell$ at the final time.

An attempt to solve this problem without relying on the strong inequality $\ell \ll 1$ would be an interesting endeavor. Such an extension is not required in the context of regularization of the single-point density. On the other hand, it would make an interesting connection to the statistics of accumulated current of matter or energy in a specified region of space [6, 7]. There is also an interesting formal analogy between the setting with arbitrary ℓ and the problem of finding the joint distribution of two accumulated currents in the Simple Symmetric Exclusion Process. The latter problem has been recently formulated in terms of the ISM (for the nonlinear Schrödinger equation rather than for the DNLS), and a possible approach to the solution has been explored [48].

In conclusion, a growing list of field-theoretical large-deviation problems have been successfully solved with the aid of the ISM in the last 3 years [10, 12–15, 41, 42]. However, this work appears to be the first instance where the ISM has been combined with a perturbation approach exploiting a small parameter (in this case ℓ), unrelated to a Lagrange multiplier. We believe that this approach holds significant promise.

Acknowledgments

We are very grateful to N. R. Smith for a critical reading of the paper and insightful comments. We also thank A. Grabsch and O. Bénichou for attracting our attention to their recent work [48]. This research was supported by the US-Israel Binational Science Foundation through Grant No. 2020193 (E.B.) and by the Israel Science Foundation through Grant 1499/20 (B.M.).

-
- [1] H. Spohn, *Large Scale Dynamics of Interacting Particles* (Springer, New York, 1991).
 - [2] T. M. Liggett, *Stochastic Interacting Systems: Contact, Voter, and Exclusion Processes* (Springer, New York, 1999).
 - [3] C. Kipnis and C. Landim, *Scaling Limits of Interacting Particle Systems* (Springer, New York, 1999).
 - [4] P. L. Krapivsky, S. Redner, and E. Ben-Naim, *A Kinetic View of Statistical Physics* (Cambridge University Press, Cambridge, UK, 2010).
 - [5] L. Bertini, A. De Sole, D. Gabrielli, G. Jona-Lasinio, and C. Landim, *Rev. Mod. Phys.* **87**, 593 (2015).
 - [6] B. Derrida and A. Gerschenfeld, *J. Stat. Phys.* **136**, 1 (2009).
 - [7] B. Derrida and A. Gerschenfeld, *J. Stat. Phys.* **137**, 978 (2009).
 - [8] T. Imamura, K. Mallick, and T. Sasamoto, *Phys. Rev. Lett.* **118**, 160601 (2017).
 - [9] T. Imamura, K. Mallick, and T. Sasamoto, *Commun. Math. Phys.* **384**, 1409 (2021).
 - [10] E. Bettelheim, N. R. Smith, and B. Meerson, *Phys. Rev. Lett.* **128**, 130602 (2022).
 - [11] A. Grabsch, A. Poncet, P. Rizkallah, P. Illien, and O. Bénichou, *Sci. Adv.* **8**, 5043 (2022).
 - [12] K. Mallick, H. Moriya, and T. Sasamoto, *Phys. Rev. Lett.* **129**, 040601 (2022).
 - [13] E. Bettelheim, N. R. Smith, and B. Meerson, *J. Stat. Mech.* (2022) 093103.
 - [14] A. Krajenbrink and P. Le Doussal, *Phys. Rev. E* **107**, 014137 (2023).
 - [15] E. Bettelheim and B. Meerson, *Phys. Rev. E* **110**, 014101 (2024).

- [16] C. Kipnis, C. Marchioro and E. Presutti, *J. Stat. Phys.* **27**, 65 (1982).
- [17] L. Bertini, A. De Sole, D. Gabrielli, G. Jona-Lasinio, and C. Landim, *Phys. Rev. Lett.* **94**, 030601 (2005).
- [18] L. Bertini, D. Gabrielli, and J. L. Lebowitz, *J. Stat. Phys.* **121**, 843 (2005).
- [19] T. Bodineau and B. Derrida, *Phys. Rev. E* **72**, 066110 (2005).
- [20] V. Lecomte, A. Imparato, and F. van Wijland, *Prog. Theor. Phys. Suppl.* **184**, 276 (2010).
- [21] J. Tailleur, J. Kurchan, and V. Lecomte, *Phys. Rev. Lett.* **99**, 150602 (2007); *J. Phys. A: Math. Theor.* **41** 505001 (2008).
- [22] P. L. Krapivsky and B. Meerson, *Phys. Rev. E* **86**, 031106 (2012).
- [23] P. I. Hurtado and P. L. Garrido, *Phys. Rev. Lett.* **107**, 180601 (2011).
- [24] A. Prados, A. Lasanta, and P. I. Hurtado, *Phys. Rev. E* **86**, 031134 (2012).
- [25] B. Meerson and P. V. Sasorov, *J. Stat. Mech.* (2013) P12011.
- [26] M. A. Peletier, F. H. J. Redig, and K. Vafayi, *J. Math. Phys.* **55**, 093301 (2014).
- [27] L. Zarfaty and B. Meerson, *J. Stat. Mech.* (2016) 033304.
- [28] O. Shpielberg, Y. Don, and E. Akkermans, *Phys Rev E* **95**, 032137 (2017).
- [29] C. Gutiérrez-Ariza and P. I. Hurtado, *J. Stat. Mech.* (2019) 103203.
- [30] R. Frassek, C. Giardinà, and J. Kurchan, *SciPost Phys.* **9**, 054 (2020).
- [31] A. Grabsch, A. Poncet, P. Rizkallah, P. Illien, and O. Bénichou, *Sci. Adv.* **8**, issue 12 (2022).
- [32] I. Corwin, *Random Matrices: Theory Appl.* **01**, 1130001 (2012).
- [33] H. Spohn, in *Stochastic Processes and Random Matrices*, edited by G. Schehr, A. Altland, Y. V. Fyodorov, and L. F. Cugliandolo, Lecture Notes of the Les Houches Summer School Vol. 104 (Oxford University Press, Oxford, 2015).
- [34] J. Quastel and H. Spohn, *J. Stat. Phys.* **160**, 965 (2015).
- [35] K. A. Takeuchi, *Physica A* **504**, 77 (2018).
- [36] I. V. Kolokolov and S. E. Korshunov, *Phys. Rev. B* **75**, 140201(R) (2007); **78**, 024206 (2008); *Phys. Rev. E* **80**, 031107 (2009).
- [37] B. Meerson, E. Katzav, and A. Vilenkin, *Phys. Rev. Lett.* **116**, 070601 (2016).
- [38] M. Janas, A. Kamenev and B. Meerson, *Phys. Rev. E* **94**, 032133 (2016).
- [39] P. V. Sasorov, B. Meerson and S. Prolhac, *J. Stat. Mech.* (2017) 063203.
- [40] N. R. Smith and B. Meerson, *Phys. Rev. E* **97**, 052110 (2018).
- [41] A. Krajenbrink and P. Le Doussal, *Phys. Rev. Lett.* **127**, 064101 (2021).
- [42] A. Krajenbrink and P. Le Doussal, *Phys. Rev. E* **105**, 054142 (2022).
- [43] M. Kardar, G. Parisi, and Y.-C. Zhang, *Phys. Rev. Lett.* **56**, 889 (1986).
- [44] J. Krug, *Adv. Phys.* **46**, 139 (1997).
- [45] N. R. Smith, B. Meerson, and P. V. Sasorov *Phys. Rev. E* **95**, 012134 (2017).
- [46] F. D. Cunden, P. Facchi, and P. Vivo, *J. Phys. A: Math. Theor.* **49**, 135202 (2016).
- [47] D. J. Kaup and A. C. Newell, *J. Math. Phys.* **19**, 798 (1978).
- [48] A. Grabsch, P. Rizkallah, and O. Bénichou, *SciPost Phys.* **16**, 016 (2024).